

Z Patch Antenna Embedded in Superstrates Anisotropic Media

Adnan Affandi¹, Mamdoh Gharbi¹, Abdullah Dobaie¹

¹(Department of Electrical and Computer, Engineering/ King Abdul Aziz University, Saudi Arabian)

Abstract: Z shape of Microstrip patch antenna embedded in superstrate uniaxial Anisotropic layers is presented. The Anisotropic effects has been enhanced the patch characteristics like directivity and gain. The formulation of the canonical problem of determining the field produced by impressed point electric (or magnetic) current sources in the presence of a multilayered uniaxially anisotropic medium, where the sources and observation points are assumed to be in any layer is investigated via plane wave spectral integral representation of the dyadic Green's function of the layered medium. The radiation field has been analyzed analytically via matlab Code than compared with CNT Studio Simulation, and the results is good agreement.

Keywords: Anisotropic Superstrate, Patch Antenna, Gain, Directivity, Return loss.

I. Introduction

Printed circuit antennas have received much attention since 1953[1]. These antennas are popular due to their attractive features and many advantages, including low profile, light weight, conformity to a given surface, low cost, easy integration with microstrip circuitry, and high reliability. Since then, this technology has been under continuous growth. A simple method for analysis is to approximate a rectangular patch as is to two parallel narrow radiating slots separated by some distance[2]. Although the transmission line model gives a simple formula for the input impedance and resonant frequency, it suffers from some serious drawbacks. It can only be applied to the rectangular shape patches, so other patch configurations cannot be analyzed by this model. A fringing factor must be empirically determined in this model. It ignores the field variation along the radiating edge, and also ignores the surface wave effects. To overcome most of these difficulties of approximate approaches described above, the moment method (MM) solution of this class of microstrip structures has been proposed by several authors [3,4]. Many materials used as substrates for printed circuits antennas or integrated microwave circuits exhibit dielectric anisotropy which either introduced during the manufacturing process or occurs naturally in the material. Designing patch antenna required a precise knowledge of material dielectric constant. Because of variations in ϵ for many material batches, an errors in printing patches design is introduced and reduced it repeatability. Anisotropy serves to improve circuit performance in some applications [5]. To protect patch antenna from environmental hazards, we use Superstrate (cover) dielectric layers. Whether a cover layer is naturally formed or imposed by design, it may affect adversely the antenna basic performance characteristics, such as gain and radiation resistance. For this reason, it is important to analyze superstrate effects so that the printed-circuit antenna performance can be predicted with higher accuracy.[6] Also, better understanding of the cover parameters may be implemented to advantage in the enhancement of the printed-circuit antenna performance.

In this study, the formulation of the canonical problem of determining the field produced by impressed point electric (or magnetic) current sources in the presence of a multilayered uniaxially anisotropic medium, where the sources and observation points are assumed to be in any layer is presented. The formal solution of the problem is obtained via plane wave spectral integral representation of the dyadic Green's function of the layered medium. The formulation decomposes the dyadic Green's function into TE and TM waves and expresses it in terms of Weyl-type integrals. Recursion relations for appropriately defined reflection and transmission coefficients are presented. Also, the plane wave spectral form of the dyadic Green's function is expressed in terms of the usual Sommerfeld form integrals.

II. Dyadic Green's Function for Uniaxially Anisotropic Layered Media

Consider the layered medium shown in Fig. 1 with impressed sources located in an arbitrary layer (j). The layers are assumed to be uniaxial in both Anisotropic ϵ and μ . That is

$$\bar{\bar{\epsilon}}_j = \begin{bmatrix} \epsilon_j & 0 & 0 \\ 0 & \epsilon_j & 0 \\ 0 & 0 & \epsilon_{jz} \end{bmatrix} \quad (1)$$

$$\bar{\bar{\mu}}_j = \begin{bmatrix} \mu_j & 0 & 0 \\ 0 & \mu_j & 0 \\ 0 & 0 & \mu_{jz} \end{bmatrix} \quad (2)$$

where $\bar{\bar{\epsilon}}_j$ and $\bar{\bar{\mu}}_j$ are the permittivity and permeability tensors, respectively.

For an impressed electric source located in the layer (j), the wave equation for in the layer (i) is given by

$$\nabla \times \bar{\bar{\kappa}}_i \cdot \nabla \times \bar{E}_i(\bar{r}) - \omega^2 \bar{\bar{\epsilon}}_i \cdot \bar{E}_i(\bar{r}) = i\omega \bar{J}_j(\bar{r})\delta_{ij} \quad (3)$$

where $\bar{\bar{\kappa}}_i = \bar{\bar{\mu}}_i^{-1}$, and δ_{ij} is the Kronecker delta.

The dyadic Green's function $\bar{\bar{G}}_{ij}(\bar{r}, \bar{r}')$ for the uniaxially anisotropic layered medium satisfy the following equation

$$\nabla \times \bar{\bar{\kappa}}_i \cdot \nabla \times \bar{\bar{G}}_{ij}(\bar{r}, \bar{r}') - \omega^2 \bar{\bar{\epsilon}}_i \cdot \bar{\bar{G}}_{ij}(\bar{r}, \bar{r}') = \begin{cases} 0 & , i \neq j \\ \bar{I} \delta(\bar{r} - \bar{r}') & , i = j \end{cases} \quad (4)$$

The electric field \bar{E}_i is given by

$$\bar{E}_i(\bar{r}) = i\omega \iiint_{V_j} \bar{\bar{G}}_{ij}(\bar{r}, \bar{r}') \cdot \bar{J}_j(\bar{r}') dV' \quad (5)$$

and V_j is the volume included by the sources in layer (j).

The dyadic Green's function $\bar{\bar{G}}_{ij}$ satisfy the following boundary conditions

$$\hat{z} \times \bar{\bar{G}}_{ij} = \hat{z} \times \bar{\bar{G}}_{(i+1)j} \quad (6)$$

$$\hat{z} \times \bar{\bar{\kappa}}_i \cdot \nabla \times \bar{\bar{G}}_{ij} = \hat{z} \times \bar{\bar{\kappa}}_{(i+1)} \cdot \nabla \times \bar{\bar{G}}_{(i+1)j} \quad (7)$$

at the interfaces $z_i = -d_i$ ($i = 0, \dots, n$). In the layer (j) (source), the dyadic Green's function $\bar{\bar{G}}_{ij}$ can be expressed as a superposition of the unbounded dyadic Green's function $\bar{\bar{G}}^{(p)}$ due to the primary excitation and a scattered dyadic Green's function $\bar{\bar{G}}_{ij}^{(s)}$. Hence for any layer (i)

$$\bar{\bar{G}}_{ij} = \bar{\bar{G}}^{(p)} + \bar{\bar{G}}_{ij}^{(s)} \quad (8)$$

where $\bar{\bar{G}}_{ij}^{(s)}$ satisfies the homogeneous equation

$$\nabla \times \bar{\bar{\kappa}}_i \cdot \nabla \times \bar{\bar{G}}_{ij}^{(s)}(\bar{r}, \bar{r}') - \omega^2 \bar{\bar{\epsilon}}_i \cdot \bar{\bar{G}}_{ij}^{(s)}(\bar{r}, \bar{r}') = 0 \quad (9)$$

When the impressed sources are magnetic, we have

$$\hat{H}_i(\bar{r}) = i\omega \iiint_{V_j} \bar{\bar{\Gamma}}_{ij}(\bar{r}, \bar{r}') \cdot \bar{M}_j(\bar{r}') dV' \quad (10)$$

where $\bar{\bar{\Gamma}}_{ij}$ is a magnetic type dyadic Green's function dual to $\bar{\bar{G}}_{ij}$ and \bar{M} is the magnetic current distribution.

$\bar{\bar{\Gamma}}_{ij}$ satisfy dual boundary conditions to Eq. 6 and Eq. 7. We can express the scattered dyadic Green's function $\bar{\bar{G}}_{ij}^{(s)}(\bar{r}, \bar{r}')$ in terms of the following two-dimensional Fourier transform:

$$\bar{\bar{G}}_{ij}^{(s)}(\bar{r}, \bar{r}') = \frac{1}{(2\pi)^2} \int \int_{-\infty}^{\infty} d\bar{k}_s \tilde{\bar{G}}_{ij}^{(s)}(\bar{k}_s, z, z') e^{i\bar{k}_s \cdot (\bar{r}_s - \bar{r}'_s)} \quad (11)$$

Substituting in Eq. 8, we get

$$\bar{L}_{e(i)}(\tilde{\nabla}_z) \cdot \bar{\bar{G}}_{ij}^{(s)}(\bar{k}_s, z, z') = 0 \quad (12)$$

where $\bar{L}_{e(i)}(\tilde{\nabla}_z)$ is a dyadic operator given by

$$\bar{\bar{L}}_{e(i)}(\tilde{\nabla}_z) = (\tilde{\nabla}_z \times \bar{\bar{\kappa}}_i \cdot \tilde{\nabla} \times \bar{\bar{I}} - \omega^2 \bar{\bar{\epsilon}}_j) \tag{13}$$

and

$$\tilde{\nabla}_z = ik_s \bar{\bar{z}} + \hat{z} \frac{d}{dz} \tag{14}$$

From Eq. 13, the transformed operator can be written explicitly as

$$\bar{\bar{L}}_{e(i)}(\tilde{\nabla}_z) = \begin{bmatrix} -\frac{1}{\mu_i} \frac{d^2}{dz^2} + \frac{k_y^2}{\mu_{iz}} - \omega^2 \epsilon_i & -\frac{1}{\mu_{iz}} k_x k_y & \frac{i}{\mu_i} k_x \frac{d}{dz} \\ -\frac{1}{\mu_{iz}} k_x k_y & -\frac{1}{\mu_i} \frac{d^2}{dz^2} + \frac{k_x^2}{\mu_{iz}} - \omega^2 \epsilon_i & \frac{i}{\mu_i} k_y \frac{d}{dz} \\ \frac{i}{\mu_i} k_x \frac{d}{dz} & \frac{i}{\mu_i} k_y \frac{d}{dz} & \frac{k_s^2}{\mu_i} - \omega^2 \epsilon_{iz} \end{bmatrix} \tag{15}$$

Using Eq. 12 and Eq. 15, it can be shown that all the components of $\bar{\bar{G}}_{ij}^{(s)}$ satisfy the same differential equation given by [7]

$$\left\{ \det \bar{\bar{L}}_{e(i)}(\tilde{\nabla}_z) \right\} G_{\alpha\nu(ij)}^{(s)} = 0, \quad \alpha, \nu = 1, 2, 3$$

where $G_{\alpha\nu(ij)}^{(s)} = [\bar{\bar{G}}_{ij}^{(s)}]_{\alpha\nu}$ and $\left\{ \det \bar{\bar{L}}_{e(i)}(\tilde{\nabla}_z) \right\}$ is determinant of the operator $\bar{\bar{L}}_{e(i)}(\tilde{\nabla}_z)$. Then,

$$\left\{ \det \bar{\bar{L}}_{e(i)}(\tilde{\nabla}_z) \right\} = -\frac{\omega^2 \epsilon_{iz}}{\mu_i^2} \left[\frac{d^2}{dz^2} + (k_{iz}^{(e)})^2 \right] \left[\frac{d^2}{dz^2} + (k_{iz}^{(h)})^2 \right] \tag{16}$$

where

$$(k_{iz}^{(h)})^2 = k_i^2 - \frac{\mu_i}{\mu_{iz}} k_s^2 \tag{17}$$

$$(k_{iz}^{(e)})^2 = k_i^2 - \frac{\epsilon_i}{\epsilon_{iz}} k_s^2 \tag{18}$$

and $k_i^2 = \omega^2 \epsilon_i \mu_i$.

Hence, we may define two possible solution to $G_{\alpha\nu(ij)}^{(s)}$ governed by

$$\left[\frac{d^2}{dz^2} + (k_{iz}^{(h)})^2 \right] G_{\alpha\nu(ij)}^{(h)} = 0, \quad \alpha, \nu = 1, 2, 3 \tag{19}$$

$$\left[\frac{d^2}{dz^2} + (k_{iz}^{(e)})^2 \right] G_{\alpha\nu(ij)}^{(e)} = 0, \quad \alpha, \nu = 1, 2, 3 \tag{20}$$

Using Eq. 19, Eq 20 Eq. 12, and Eq. 15 it can easily be shown that

$$G_{3\nu(ij)}^{(h)} = 0 \tag{21}$$

$$k_x G_{1\nu(ij)}^{(h)} + k_y G_{2\nu(ij)}^{(h)} = 0, \quad \nu = 1, 2, 3 \tag{22}$$

Hence $G_{\alpha\nu(ij)}^{(h)}$ satisfying Eq. 19 represent the electric field of a TE field. Similarly, it is found that

$$k_y G_{1\nu(ij)}^{(e)} - k_x G_{2\nu(ij)}^{(e)} = 0, \quad \nu = 1, 2, 3 \tag{23}$$

$$G_{3\nu(ij)}^{(e)} = \frac{-i\epsilon_j}{\epsilon_{iz} (k_{iz}^{(e)})^2} \left(k_x \frac{d}{dz} G_{1\nu(ij)}^{(e)} + k_y \frac{d}{dz} G_{2\nu(ij)}^{(e)} \right), \quad \nu = 1, 2, 3 \tag{24}$$

$G_{\alpha\nu(ij)}^{(e)}$ represent the electric field of a TM wave. And $\bar{\bar{G}}_{(ij)}^{(s)}$ represent the superposition of TE Wave that is

$$\bar{\bar{G}}_{(ij)}^{(s)} = \bar{\bar{G}}_{(ij)}^{(h)} + \bar{\bar{G}}_{(ij)}^{(e)} \tag{25}$$

In an unbounded region with parameters $\overline{\overline{\epsilon}}_j$ and $\overline{\overline{\mu}}_j$ given by Eq. 1 and Eq. 2, respectively, the dyadic Green's function satisfy the following wave equation

$$\nabla \times \overline{\overline{\kappa}}_j \cdot \nabla \times \overline{\overline{G}}^{(p)}(\overline{r}, \overline{r}') - \omega^2 \overline{\overline{\epsilon}}_j \cdot \overline{\overline{G}}^{(p)}(\overline{r}, \overline{r}') = \overline{\overline{I}} \delta(\overline{r} - \overline{r}') \quad (26)$$

Starting from Eq. 26 and expressing $\overline{\overline{G}}^{(p)}(\overline{r}, \overline{r}')$ as an integral representation by means of its three-dimensional Fourier transform, we arrive at

$$\overline{\overline{G}}^{(p)}(\overline{r}, \overline{r}') = \frac{-1}{\omega^2 \epsilon_{jz}} \hat{z} \hat{z} \delta(\overline{r} - \overline{r}') + \frac{i\mu_j}{8\pi^2} \int_{-\infty}^{\infty} \int_{-\infty}^{\infty} d\overline{k}_s e^{i\overline{k}_s \cdot (\overline{r}_s - \overline{r}'_s)} \begin{cases} \left[\frac{1}{k_{jz}^{(h)}} \hat{h} \hat{h} e^{ik_{jz}^{(h)}(z-z')} + \frac{1}{k_{jz}^{(e)}} \hat{v}(k_{jz}^{(e)}) \hat{v}(k_{jz}^{(e)}) e^{ik_{jz}^{(e)}(z-z')} \right] & , z > z' \\ \left[\frac{1}{k_{jz}^{(h)}} \hat{h} \hat{h} e^{-ik_{jz}^{(h)}(z-z')} + \frac{1}{k_{jz}^{(e)}} \hat{v}(-k_{jz}^{(e)}) \hat{v}(-k_{jz}^{(e)}) e^{-ik_{jz}^{(e)}(z-z')} \right] & , z < z' \end{cases} \quad (27)$$

where

$$\hat{h} = \hat{h}(k_{jz}^{(h)}) = \hat{h}(-k_{jz}^{(h)}) = \frac{1}{k_s} (\overline{k}_s \times \hat{z}) \quad (28)$$

and

$$\hat{v}(\pm k_{jz}^{(e)}) = \frac{1}{k_j} \hat{h} \times \left(\frac{\epsilon_j}{\epsilon_{jz}} \overline{k}_s \pm \hat{z} k_{jz}^{(e)} \right) \quad (29)$$

\hat{h} is a unit vector in the direction of the electric field for TE waves and \hat{v} is a vector in the direction of the electric field for TM waves. In the above the resolution of the field into TE and TM waves follows easily by collecting together terms containing $k_{jz}^{(h)}$ and $k_{jz}^{(e)}$, respectively.

The $\overline{\overline{G}}_{00}(\overline{r}, \overline{r}')$ will be driven. Thus, if we consider the sources to be located in the upper half-space of the layered medium, $\overline{\overline{G}}_{00}$ can be represented as a superposition of $\overline{\overline{G}}^{(p)}$ given by Eq. 27 and a scattered dyadic Green's function $\overline{\overline{G}}^{(s)}$ which is the contribution from the layered medium. Thus, we have

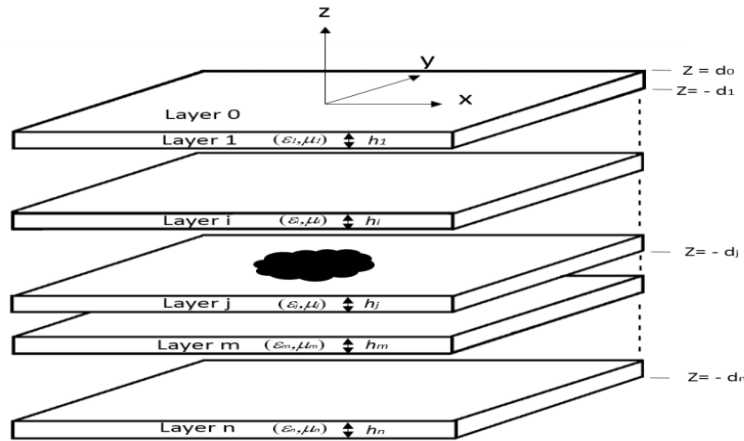
$$\overline{\overline{G}}_{00}(\overline{r}, \overline{r}') = \hat{z} \hat{z} \frac{-\delta(\overline{r} - \overline{r}')}{\omega^2 \epsilon_{0z}} + \frac{i\mu_0}{8\pi^2} \int_{-\infty}^{\infty} \int_{-\infty}^{\infty} d\overline{k}_s e^{i\overline{k}_s \cdot (\overline{r}_s - \overline{r}'_s)} \overline{\overline{g}}_{00}(\overline{k}_s, z; z') \quad (30)$$

where for $z > z'$:

$$\overline{\overline{g}}_{00}(\overline{k}_s, z; z') = \left\{ \frac{1}{k_{0z}^{(h)}} \left[\hat{h}(k_{0z}^{(h)}) \hat{h}(k_{0z}^{(h)}) e^{i\overline{k}_{0z}^{(h)}(z_0 - z'_0)} + R_{\cap 0}^{TE} \hat{h}(k_{0z}^{(h)}) \hat{h}(-k_{0z}^{(h)}) e^{i\overline{k}_{0z}^{(h)}(z_0 + z'_0)} \right] \right. \\ \left. + \frac{1}{k_{0z}^{(e)}} \left[\hat{v}(k_{0z}^{(e)}) \hat{v}(k_{0z}^{(e)}) e^{i\overline{k}_{0z}^{(e)}(z_0 - z'_0)} + R_{\cap 0}^{TM} \hat{v}(k_{0z}^{(e)}) \hat{v}(-k_{0z}^{(e)}) e^{i\overline{k}_{0z}^{(e)}(z_0 + z'_0)} \right] \right\} \quad (31)$$

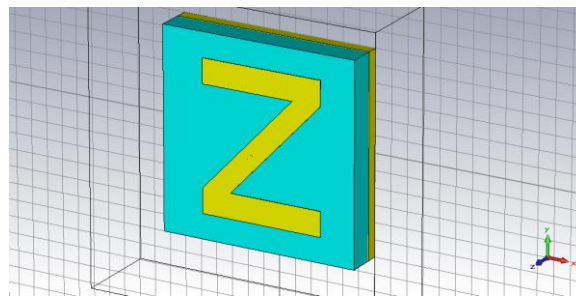
and for $z < z'$:

$$\overline{\overline{g}}_{00}(\overline{k}_s, z; z') = \left\{ \frac{1}{k_{0z}^{(h)}} \left[\hat{h}(-k_{0z}^{(h)}) \hat{h}(-k_{0z}^{(h)}) e^{-i\overline{k}_{0z}^{(h)}(z_0 - z'_0)} + R_{\cap 0}^{TE} \hat{h}(-k_{0z}^{(h)}) \hat{h}(k_{0z}^{(h)}) e^{i\overline{k}_{0z}^{(h)}(z_0 + z'_0)} \right] \right. \\ \left. + \frac{1}{k_{0z}^{(e)}} \left[\hat{v}(-k_{0z}^{(e)}) \hat{v}(-k_{0z}^{(e)}) e^{-i\overline{k}_{0z}^{(e)}(z_0 - z'_0)} + R_{\cap 0}^{TM} \hat{v}(-k_{0z}^{(e)}) \hat{v}(k_{0z}^{(e)}) e^{i\overline{k}_{0z}^{(e)}(z_0 + z'_0)} \right] \right\} \quad (32)$$



III. Results And Discussion

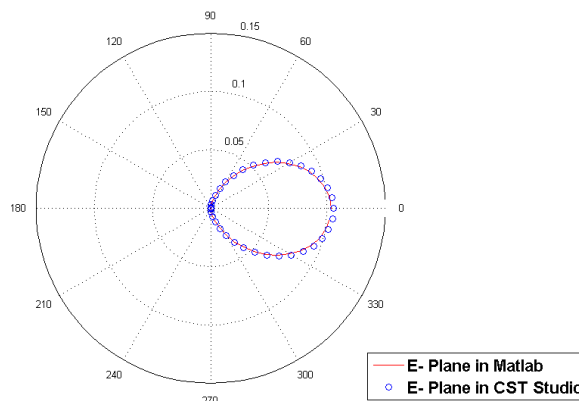
Z patch numerical results embedded in anisotropic superstrate structures is shown in Figure 2. The effects of anisotropy of Superstrate layers in S-parameters, Axial Ratio, Directivity and gain are investigated. To simulate the Far Field Radiation of Z Patch Antenna, a Matlab program is written. For Validation propose simulation software CST STUDIO SUITE® is used. The compered result between the Two programs was good similarity. A microstrip Z patch of length $L_p = 7$ mm and width $W = 5.5$ mm on the top of Rogers an isotropic substrate of permittivity $\epsilon_r = 3.38$, and thickness $h_s = 1.5$ mm. The Ground plate of rectangular shape with length $L = 12$ mm and $W = 8$ mm.. The Z patch is fed with coaxial probe. The following anisotropic superstrates are used: piroltyc boron nitride, or pbn $\epsilon_{xx} = 5.12$; $\epsilon_{zz} = 3.4$), sapphire ($\epsilon_{xx} = 9.4$; $\epsilon_{zz} = 11.6$), Epsilam-10 ($\epsilon_{xx} = 13$; $\epsilon_{zz} = 10.6$). For $\epsilon_r = 1$ (vacuum or Air) use Foam flakes $\epsilon_r = 1.1$, which is good approximation.



3.1 E-Plane Radiation of Z Patch with one Superstrate Anisotropic layer

The Anisotropic Superstrate effect for Z Patch Antenna is conducted. The Superstrate Layer assumed to be anisotropic media with permittivity Epsilam-10 ($\epsilon_{xx} = 13$; $\epsilon_{zz} = 10.6$). The E- Plane Radiation of Z Patch antenna fed by Coaxial Cable was shown in Figure 3.

E-plane radiation plot of B Patch Antenna with one superstrate Anisotropic media



The CST Simulating result almost identical to the theoretical model.

3.2 Farfield Directivities and gainsof Z patch without any superstrate

A Z patch without any superstrate was considered. Fig. 1,shows, the circuit of Z patch.

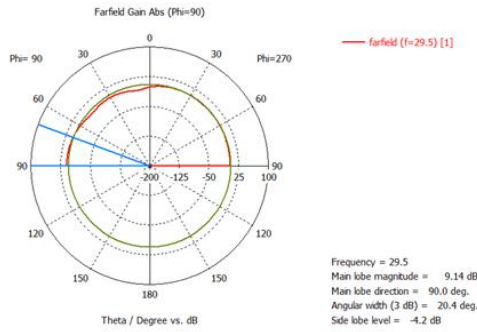


Figure 2. Directivity of Z Patch at Fr=29.5 GHz

F GHz	Directivity dBi	Gain dBi
27.5	8.45	8.41
29.5	9.21	9.14
31	5.54	5.49
33	4.84	4.73
35	8.17	8.06
39	4.17	4.07
41	5.8	5.67
43	3.88	3.68
45	1.93	1.7
47	5.93	5.79
49	6.57	6.47

Table 1, Directivities and gains of Z PatchAntenna without Superstrate

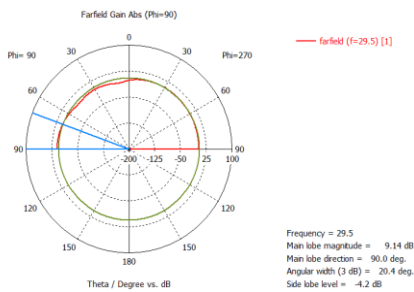


Figure 3. Gain of Z Patch at Fr=29.5 GHz

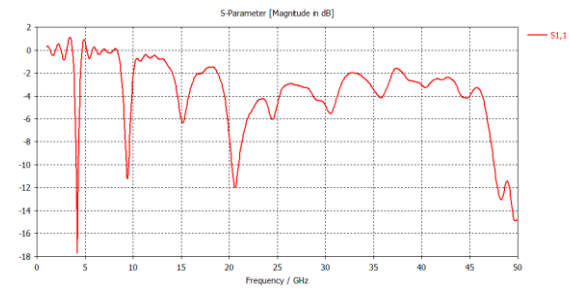


Figure 4, S11 of Z Patch Antenna

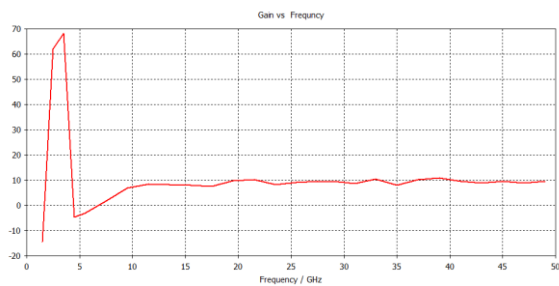


Figure 5. Gain over Frequency of Z Patch Antenna

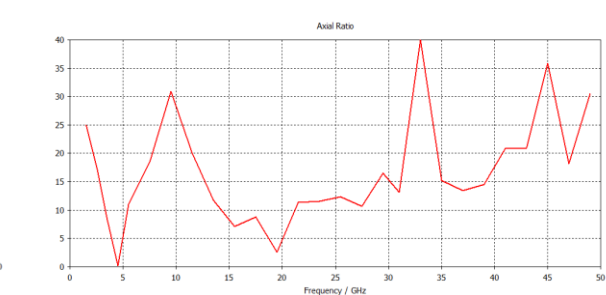


Figure 6. Axial Ratio of B Patch Antenna

CST Studio Suite designs the Z patch (Fig. 1). Fig.4. Shows S11 for this configuration.It is clear from Fig.2, Z patch directivity is 9.21dBi.The gain of that patch is 9.14 dBi as shown in Fig. 3. Gain over Frequency is shown in Fig. 5, where Axial Ratio shown in Fig. 6.

3.3. Farfield Directivities and gains of Z patch with one superstrate layer

Table 2 Directivities and gains of Z Patch Antenna with one Anisotropic Superstrate layer, $\epsilon_{xx} = 5.12$; $\epsilon_{zz} = 3.4$

F GHz	Directivity dBi	Gain dBi
27.5	5.47	5.42
29.5	5.86	5.76
31	5.67	5.61
33	7.04	6.97
35	3.07	2.99
37	7.7	7.58
39	9.14	9.06
43	7.7	7.57
45	6.63	6.49
47	5.93	5.84
49	5.41	5.29

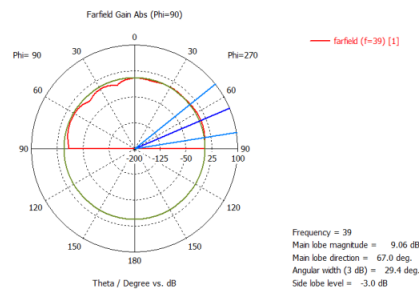


Figure 7. Directivity of Z Patch at F=39 GHz with one Anisotropic Superstrate layer, $\epsilon_{xx} = 5.12$; $\epsilon_{zz} = 3.4$

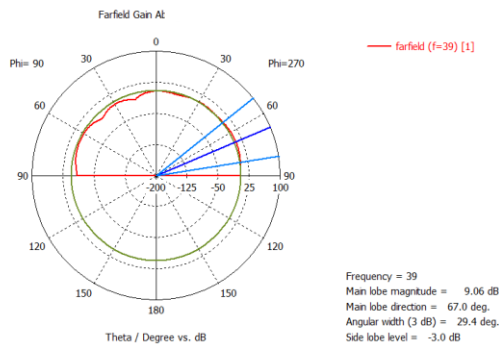


Figure 8. Gain of Z Patch at F=39 GHz with one Anisotropic Superstrate layer, $\epsilon_{xx} = 5.12$; $\epsilon_{zz} = 3.4$

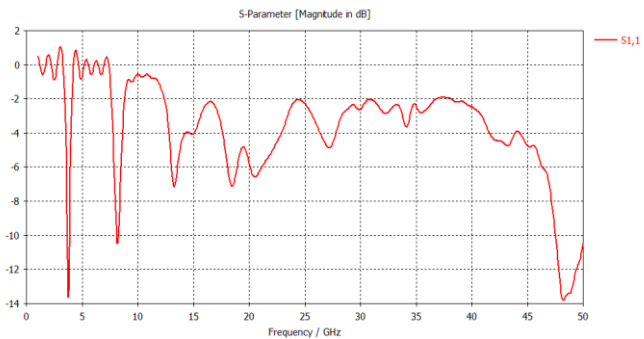


Figure 9. S11 of Z Patch Antenna with one Anisotropic Superstrate layer, $\epsilon_{xx} = 5.12$; $\epsilon_{zz} = 3.4$

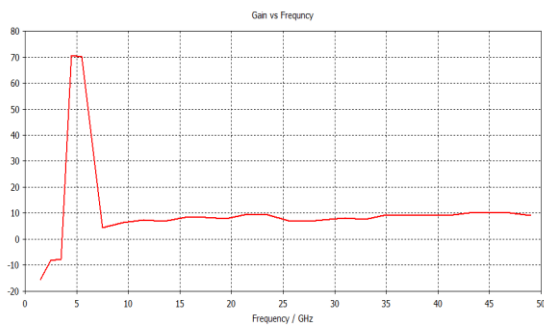


Figure 10. Gain over Frequency of Z Patch Antenna

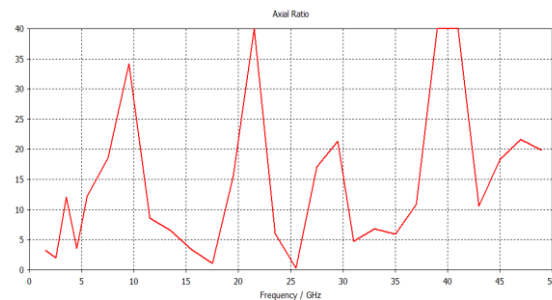


Figure 11. Axial Ratio of B Patch Antenna with one Anisotropic Superstrate layer, $\epsilon_{xx} = 5.12$; $\epsilon_{zz} = 3.4$

Fig. 7. Shows the directivity for Z patch with pirolytic boron nitride, or pbn $\epsilon_{xx} = 5.12$; $\epsilon_{zz} = 3.4$ superstrate is less than Z patch without Superstrate. In addition, the gain also decreased if adding a superstrate. Fig, 9, shows S11.Gain over Frequency is shown in Fig. 10, where Axial Ratio shown in Fig. 11.

3.4. Farfield Directivities and gains of Z patch with two superstrate layers

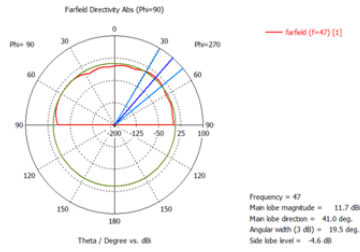


Figure 12. Directivity of Z Patch at F=47 GHz with two Anisotropic Superstrate layers, and $\epsilon_{1_{xx}} = 9.4$; $\epsilon_{1_{zz}} = 11.6$ (layer 2), $\epsilon_{2_{xx}} = 13$; $\epsilon_{2_{zz}} = 10.6$ (layer 2).

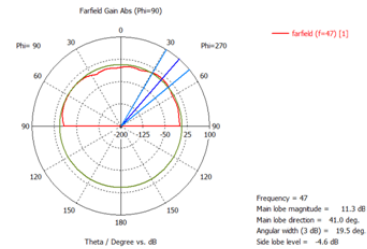


Figure 13. Gain of Z Patch at F=47 GHz with two Anisotropic Superstrate layers, and $\epsilon_{1_{xx}} = 9.4$; $\epsilon_{1_{zz}} = 11.6$ (layer 2), $\epsilon_{2_{xx}} = 13$; $\epsilon_{2_{zz}} = 10.6$ (layer 2).

F GHz	Directivity dBi	Gain dBi
27.5	9.42	9.39
29.5	7.17	6.7
31	6.26	5.97
33	6.19	6
35	6.91	6.64
37	6.82	6.75
39	5.72	5.43
41	9.87	9.83
43	8.66	8.4
45	9.21	9.07
47	11.7	11.3

Table 3 Directivities and gains of Z Patch Antenna with two Anisotropic Superstrate layers, and $\epsilon_{1_{xx}} = 9.4$; $\epsilon_{1_{zz}} = 11.6$ (layer 2), $\epsilon_{2_{xx}} = 13$; $\epsilon_{2_{zz}} = 10.6$ (layer 2).

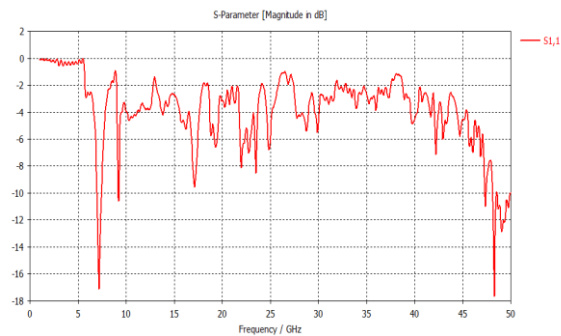


Figure 14. S11 of Z Patch at F=47 GHz with two Anisotropic Superstrate layers, and $\epsilon_{1_{xx}} = 9.4$; $\epsilon_{1_{zz}} = 11.6$ (layer 2), $\epsilon_{2_{xx}} = 13$; $\epsilon_{2_{zz}} = 10.6$ (layer 2).

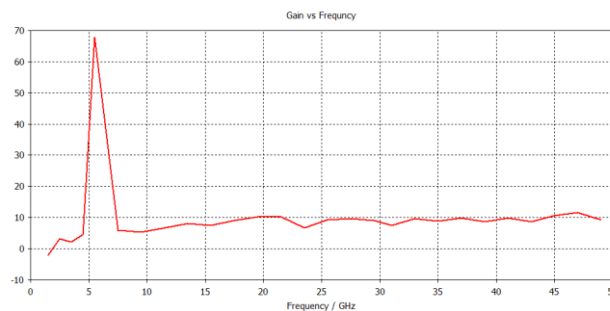


Figure 15. Gain over Frequency of B Patch Antenna with two Anisotropic Superstrate layers, and $\epsilon_{1_{xx}} = 9.4$; $\epsilon_{1_{zz}} = 11.6$ (layer 2), $\epsilon_{2_{xx}} = 13$; $\epsilon_{2_{zz}} = 10.6$ (layer 2).

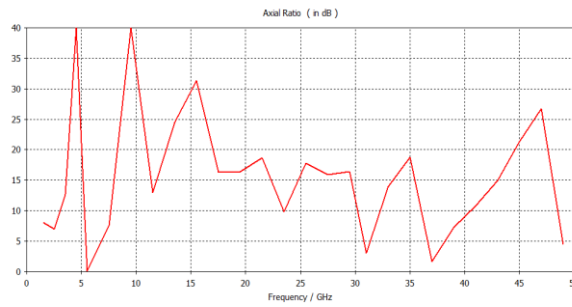


Figure 16. Axial Ratio of B Patch Antenna with two Anisotropic Superstrate layers, and $\epsilon_{1_{xx}} = 9.4$; $\epsilon_{1_{zz}} = 11.6$ (layer 2), $\epsilon_{2_{xx}} = 13$; $\epsilon_{2_{zz}} = 10.6$ (layer 2).

In this configuration, sapphire ($\epsilon_{xx} = 9.4$; $\epsilon_{zz} = 11.6$) for Superstrate 1 is used. While, Epsilam-10 ($\epsilon_{xx} = 13$; $\epsilon_{zz} = 10.6$) is used for Superstrate 2. From Fig. 12 Directivity was increased to 11.7 dBi, and the gain was 11.3 at frequency $f_r = 47$ GHz at Fig. 13. Fig. 14, shows S11. Gain over Frequency is shown in Fig. 15, where Axial Ratio shown in Fig. 16.

3.5. Farfield Directivities and gains of Z patch with three superstrate layers

F GHz	Directivity dBi	Gain dBi
27.5	8.64	8.59
29.5	5.25	4.71
31	4.16	3.89
33	4.08	3.9
35	4.85	4.58
37	4.77	4.71
39	3.77	3.54
41	9.53	9.4
43	7.12	6.71
45	8.73	8.42
47	14.6	13.5
49	3.95	3.78

Table 4. Directivities and gains of Z Patch Antenna with three Anisotropic Superstrate Layers, $\epsilon_{1_{xx}} = 9.4$; $\epsilon_{1_{zz}} = 11.6$ (layer 1) and $\epsilon_{2_{xx}} = 13$; $\epsilon_{2_{zz}} = 10.6$ (layer 2), $\epsilon_{3_{xx}} = 1$; $\epsilon_{3_{zz}} = 1$ (layer 3)

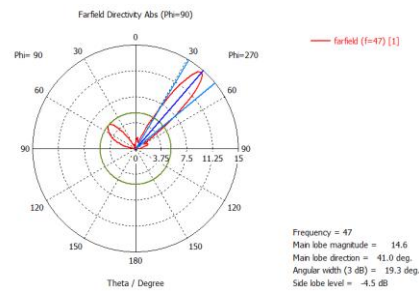


Figure 17. Directivity of Z Patch at $F=47$ GHz with three Anisotropic Superstrate Layers, $\epsilon_{1_{xx}} = 9.4$; $\epsilon_{1_{zz}} = 11.6$ (layer 1) and $\epsilon_{2_{xx}} = 13$; $\epsilon_{2_{zz}} = 10.6$ (layer 2), $\epsilon_{3_{xx}} = 1$; $\epsilon_{3_{zz}} = 1$ (layer 3)

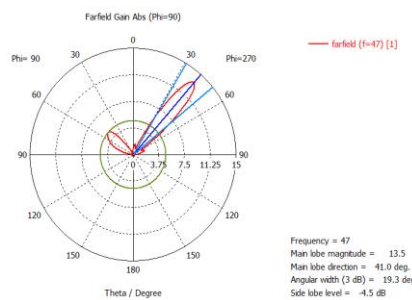


Figure 18. Gain of Z Patch at $F=47$ GHz with three Anisotropic Superstrate Layers, $\epsilon_{1_{xx}} = 9.4$; $\epsilon_{1_{zz}} = 11.6$ (layer 1) and $\epsilon_{2_{xx}} = 13$; $\epsilon_{2_{zz}} = 10.6$ (layer 2), $\epsilon_{3_{xx}} = 1$; $\epsilon_{3_{zz}} = 1$ (layer 3)

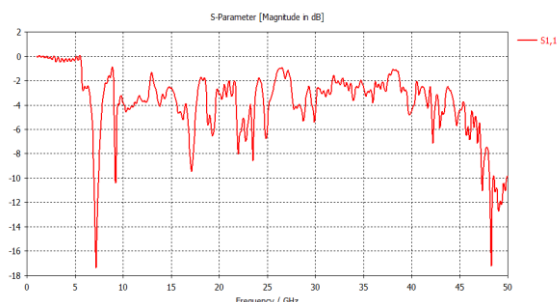


Figure 19. S11 of Z Patch at F=47 GHz with three Anisotropic Superstrate Layers, $\epsilon_{1_{xx}} = 9.4$; $\epsilon_{1_{zz}} = 11.6$ (layer 1) and $\epsilon_{2_{xx}} = 13$; $\epsilon_{2_{zz}} = 10.6$ (layer 2) , $\epsilon_{3_{xx}} = 1$; $\epsilon_{3_{zz}} = 1$ (layer 3)

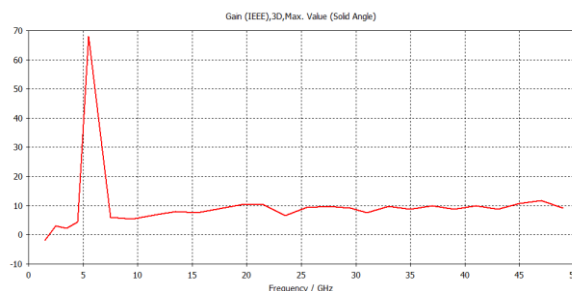


Figure 20. Gain over Frequency of B Patch Antenna withthree Anisotropic Superstrate Layers, $\epsilon_{1_{xx}} = 9.4$; $\epsilon_{1_{zz}} = 11.6$ (layer 1) and $\epsilon_{2_{xx}} = 13$; $\epsilon_{2_{zz}} = 10.6$ (layer 2) , $\epsilon_{3_{xx}} = 1$; $\epsilon_{3_{zz}} = 1$ (layer 3)

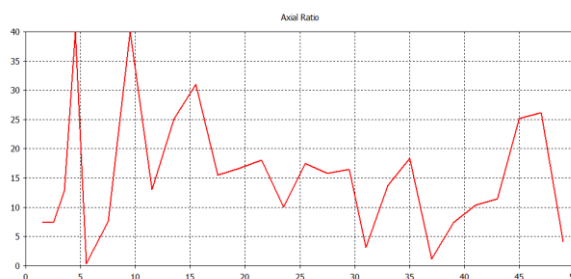


Figure 21. Axial Ratio of B Patch Antenna withthree Anisotropic Superstrate Layers, $\epsilon_{1_{xx}} = 9.4$; $\epsilon_{1_{zz}} = 11.6$ (layer 1) and $\epsilon_{2_{xx}} = 13$; $\epsilon_{2_{zz}} = 10.6$ (layer 2) , $\epsilon_{3_{xx}} = 1$; $\epsilon_{3_{zz}} = 1$ (layer 3)

In this case, sapphire ($\epsilon_{xx} = 9.4$; $\epsilon_{zz} = 11.6$), was used for the superstrate one . The Second one is), Epsilam-10 ($\epsilon_{xx} = 13$; $\epsilon_{zz} = 10.6$).The third one is Foam $\epsilon_r = 1.1$. (The Directivity equal 14.6dBi from Fig. 17. The Gain is 13.5 dBi from Fig. 18. S11 was shown in Fig. 19.

III. Conclusion

Z shape of Microstrip patch antenna embedded in Superstrate uniaxial Anisotropic layers has been investigated. The Anisotropic effects has been proved to enhance the patch characteristics like directivity and gain. The field produced by impressed point electric (or magnetic) current sources in the presence of a multilayered uniaxially anisotropic medium has been calculated via plane wave spectral integral representation of the dyadic Green's function of the layered medium. The radiation field has been analyzed analytically via matlab Code than compared with CNT Studio Simulation, and the results is good agreement. This work shows a high gain and directivity for Z patch antenna embedded in multilayers anisotropic media. Also, it shows, how the anisotropic phenomena can improve the performance of the patch antenna.

References

- [1] Nguyen, D.L, Paulson, K.S, Riley, N.G. : 'Reduced-size circularly polarised square microstrip antenna for 2.45 GHz RFID applications', IET Microwaves, Antennas & Propagation, 2012, Volume 6, Issue 1, p. 94.
- [2] Peixeiro, Custodio. : 'Microstrip patch antennas: An historical perspective of the development', Microwave & Optoelectronics Conference (IMOC), 2011 SBMO/IEEE MTT-S International, pp 684 – 688.
- [3] R. Kastner, E. Heyman, A. Sabban. : 'Spectral domain iterative analysis of single- and double-layered microstrip antennas using the conjugate gradient algorithm', IEEE Transactions on Antennas and Propagation, 1212.
- [4] E. H. Newman. : ' Strip Antennas in a Dielectric Slab', IEEE Trans. on Antennas and propagation, September 28, 1978, Vol. AP-26, No. 5, pp 647-653.
- [5] K. C. Gupta , R. Gary, I. J. Bahl. : ' Microstrip Lines & Slot Lines', Dedhams, MA Artech House , 1979, 3rdedn. 2013.
- [6] N. G. Alexopoulos and D. R. Jackson. : ' Fundamental Superstrate (Cover) Effects on Printed Circuit Antennas', IEEE Trans. on Antennas and Propagation, August 1984, Vol. AP-32, No. 8, pp 807-817.
- [7] S M. Ali, and S F. Mahmoud. : ' Electromagnetic Fields of Buried Sources in Stratified Anisotropic Media', IEEE Trans. on Antennas and Propagation, September, 1979, Vol. AP-27, No. 5, 671-678
- [8] M. Gharbi, A. Affandi, S. Ali, S. Application of The Moment Method in The Spectral Domain, *Life Science Journal*, 5,2015,1 – 23.
- [9] G. Pettis, Hertzian Dipoles and Microstrip Circuits on Arbitrarily Oriented Biaxially Anisotropic Media, *PhD Dissertation, Syracuse University, Syracuse, NY*, December, 2008.

- [10] J. Graham, Arbitrarily Oriented Biaxially Anisotropic Media: Wave Behavior and Microstrip Antennas, *PhD Dissertation, Syracuse University, Syracuse, NY*, 2012.
- [11] A. K. Verma, Input Impedance of Rectangular Microstrip Patch Antenna With Iso/Anisotropic Substrate-Superstrate, *IEEE Mic. and Wir. Lit.*, **II**, 2001, 456-458.
- [12] A. Affandi, M. Gharbi, S. Ali, Plane Wave Spectral Integral Representation of the Dyadic Greens Function of Layered Media, *Life Sci. Journal*, **4**, 2015, 164 – 174.